Pergamon

*Int. J. Heat Mass Transfer.* Vol. 37, No. 7, pp. 1165–1172, 1994

0017–9310/94 $6.00+0.00

0017–9310(93)E0043–G

# Three-equation turbulence model for prediction of the mean square temperature variance in grid-generated flows and round jets

G. MOMPEAN

Depto de Energia, Fac. de Engenharia Mecânica, Universidade Estadual de Campinas, CP 6122, Campinas, CEP 13081-970, SP, Brazil

(*Received* 7 *July* 1993 *and in final form* 20 *October* 1993)

**Abstract**—This paper presents a three-equation turbulence model for the determination of turbulent quantities, such as the mean square temperature variance, turbulence kinetic energy and its dissipation rate. The conservation equations are discretized by the finite volume method SOLA [Hirt *et al.*, Los Alamos Laboratory, Report LA-5852 (1975)]. The model is tested for a grid-generated flow and for a fairly hot axisymmetrical turbulent air jet. The results of the present calculations are compared with the experimental data of other authors. The comparison shows that the good agreement, for the thermal field, depends fundamentally on the value of the turbulent Prandtl number and the ratio of time scales of turbulent temperature and velocity field.

## 1. INTRODUCTION

THE PREDICTION of the turbulent thermal field is important for several engineering applications and for nuclear fast reactors in particular. The zones of mixture between the turbulent flows of different temperatures are places of important temperature gradients and fluctuations. It occurs in the outlet of the core of the nuclear fast reactors and in the mixture of two flows with different temperatures in the outlet of tubes. The temperature fluctuations can attack the structures by the phenomena of thermal striping.

Several authors have worked in the modeling of turbulent flow with heat transfer using second order closures. In 1978, Launder [1] give a bibliographical review and proposed closures for the unknown terms. Lemos and Sesonske [2] show the results obtained with an algebraic model applied to a flow of liquid metal inside a tube. Chung and Sung [3] present a mixed model with two algebraic equations (for the Reynolds stress and for the turbulent heat flux) and two differential equations (for the temperature fluctuation and its dissipation rate), applied to a turbulent boundary layer over a heated plate.

In order to predict temperature fluctuations in turbulent flows, a model of turbulence has been developed with three transport equations for the variance of the temperature ($\overline{\theta^2}$), the kinetic energy of turbulence ($k$) and the dissipation rate of kinetic energy ($\varepsilon$). The fluid is considered incompressible and Newtonian. The following properties, viscosity, thermal conductivity and specific heat, are considered constant. As for density, its dependence on temperature has been considered using the Boussinesq approximation.

To deal with the turbulent flow, the three variables, velocity, pressure and temperature, are divided into medium and fluctuating parts in the continuity, Navier–Stokes and energy equations. The Reynolds tensor is determined using the turbulent viscosity with the $k$–$\varepsilon$ model. The turbulent heat fluxes are determined using a turbulent diffusivity with a constant value for the turbulent Prandtl number. The equation for the temperature fluctuations is closed using the first gradient law for the term of turbulent diffusion. The ratio ($R$) of time scales of turbulent temperature and velocity fields is employed to obtain the dissipation rate of temperature fluctuations.

The finite volume method is used to solve numerically this system of differential equations. We use the principle of staggered mesh; all the scalars are treated in the center of the control volumes and the velocities are localized in the center of the faces of the control volumes. The equations are discretized in time with the semi-implicit scheme. This method is derived from SOLA [4]. The code used was the TRIO-VF/CEA, and the computer was a CRAY-1.

First, this model will be tested for the turbulent flow below a heated grid, and the numerical results obtained will be compared with the experimental results of two experiments. For the first one, we have used the experimental results for homogeneous hot turbulence below a grid of Warhaft and Lumley [5], which allows us to test the model in a configuration of constant mean temperature. The second set of experimental results for the grid turbulent flow with cross-stream temperature gradient of Sirivat and Warhaft [6], allows us to test the model where the production terms of temperature fluctuations are important.

Then, the model will be tested for the fairly hot round turbulent air jet, and the numerical results obtained will be compared with the experimental results. The measured values are obtained from

## NOMENCLATURE

- $B$ mesh size of the grid placed in the wind tunnel
- $C$ model constants
- $g$ gravity acceleration
- $G$ generation rate of turbulent energy due to buoyancy effects
- $k$ turbulent kinetic energy
- $p$ pressure
- $P$ generation rate of turbulent energy
- $R$ ratio of time scales of turbulent temperature and velocity field
- $Pr_t$ turbulent Prandtl number
- $Pr_k$ constant Prandtl number for the $k$ equation
- $R_f$ Richardson flux number
- $T$ temperature
- $T_m$ maximum temperature in the cross-section of the jet
- $T_e$ ambient temperature
- $\overline{U_i}$ averaged velocity components
- $u_i$ components of fluctuating velocity
- $W$ vertical velocity
- $Z$ vertical coordinate.

Greek symbols

- $\alpha_t$ thermal eddy diffusivity
- $\beta$ coefficient of thermal expansion
- $\varepsilon$ dissipation rate of kinetic energy of turbulence
- $\overline{\theta^2}$ variance of temperature fluctuations
- $\nu_t$ eddy viscosity
- $\rho$ density.

Bahraoui and Fulachier [7]. For this experiment, the comparisons between calculations and measured values are made in two cross-sections of the jet for: mean velocity, mean temperature, Reynolds stress and variance of temperature fluctuations.

## 2. TRANSPORT EQUATIONS FOR THE MEAN FLOW

The fluid is considered incompressible and Newtonian. For the physical properties, we take the viscosity, thermal conductivity and the specific heat as constants. For the density, the Boussinesq approach is used:

$$\rho(T) = \rho^0[1-\beta(T-T^0)] \tag{1}$$

where $\rho^0$ is the density at the reference temperature ($T^0$) and $\beta$ the volumetric expansion coefficient. The variations of density are only taken into account in the source term due to buoyancy effects in the momentum conservation equation.

To treat the turbulent flow the Reynolds decomposition is employed. It decomposes the instantaneous variables, velocities ($U_i$), temperature ($T$) and pressure ($p$) as the addition of the mean field and the fluctuating field:

$$U_i = \overline{U_i} + u'_i$$
$$p = \bar{p} + p'$$
$$T = \bar{T} + \theta. \tag{2}$$

$\overline{U_i}$, $\bar{P}$ and $\bar{T}$ represent the mean quantities of the instantaneous components; $u'_i$, $p'$, and $\theta$ their fluctuating components. Applying this decomposition to the variables in the local instantaneous equations, the governing equations for the mean velocity and temperature in turbulent flows can be written as follows.

### 2.1. *Mass conservation equation*

$$\frac{\partial \overline{U_i}}{\partial x_i} = 0. \tag{3}$$

### 2.2. *Momentum conservation equation*

$$\frac{\partial \overline{U_i}}{\partial t} + \frac{\partial}{\partial x_j}(\overline{U_j U_i}) = -\frac{\partial \bar{p}}{\rho^0 \partial x_i} + \frac{\partial}{\partial x_j}\left(\nu \frac{\partial \overline{U_i}}{\partial x_j} - \overline{u_i u_j}) + g_i(1-\beta(\bar{T}-\overline{T^0})\right). \tag{4}$$

### 2.3. *Energy conservation equation*

$$\frac{\partial \bar{T}}{\partial t} + \frac{\partial}{\partial x_i}(\overline{U_i T}) = \frac{\partial}{\partial x_i}\left(\alpha \frac{\partial \bar{T}}{\partial x_i} - \overline{u_i \theta}\right). \tag{5}$$

In this system of equations we have two additional unknowns, the Reynolds stress tensor ($\overline{u_i u_j}$) and the turbulent heat flux ($\overline{u_i \theta}$). The Reynolds stress tensor will be obtained with the turbulent model $k$–$\varepsilon$. The model using a turbulent Prandtl number will be employed to obtain the turbulent heat flux.

## 3. TURBULENCE MODEL FOR THE VELOCITY FIELD

To obtain the Reynolds stress tensor the hypothesis of an eddy viscosity ($\nu_t$) is employed. In this modeling, the proportionality between the Reynolds stress and the deformation tensor is used:

$$-\overline{u_i u_j} = \nu_t\left(\frac{\partial \overline{U_i}}{\partial x_j} - \frac{\partial \overline{U_j}}{\partial x_i}\right) - \frac{2}{3}k\delta_{ij} \tag{6}$$

where $\delta_{ij}$ is the delta Cramer operator: $\delta_{ij} = 1$ if $i = j$, and $\delta_{ij} = 0$ if $i \neq j$. The eddy viscosity is obtained from the $k$–$\varepsilon$ model, where $k$ is the turbulent kinetic energy and $\varepsilon$ its dissipation rate:

$$\nu_t = C_\mu \frac{k^2}{\varepsilon};$$

where $C_\mu = 0.09$.

3.1. *Turbulent kinetic energy* ($k$)

The equation for $k$ is written in its differential modeled form [8]:

$$\frac{Dk}{Dt} = \frac{\partial}{\partial x_j}\left(\frac{\nu_t}{Pr_k}\frac{\partial k}{\partial x_j}\right) + P + G - \varepsilon \tag{7}$$

$$P = \overline{u_i u_j}\frac{\partial \bar{U}_i}{\partial x_j}, \quad G = \beta g_i \overline{u_i \theta}, \quad Pr_k = 1.0.$$

$P$ represents the generation rate of turbulent kinetic energy due to the mean velocity gradients and $G$ the generation rate of turbulent energy due to buoyancy effects.

3.2. *Dissipation rate of turbulent kinetic energy* ($\varepsilon$)

The equation for the dissipation rate of turbulent kinetic energy is used in the following form [8]:

$$\frac{D\varepsilon}{Dt} = \frac{\partial}{\partial x_j}\left(\frac{\nu_t}{Pr_\varepsilon}\frac{\partial \varepsilon}{\partial x_j}\right) + \text{Source}(\varepsilon) \tag{8}$$

$$\text{Source}(\varepsilon) = C_{\varepsilon 1}(1 + C_{\varepsilon 3}R_f)(P+G)\frac{\varepsilon}{k} - C_{\varepsilon 2}\frac{\varepsilon^2}{k}.$$

The constant values used are taken from [8]:

$$Pr_\varepsilon = 1.3, \quad C_{\varepsilon 1} = 1.44, \quad C_{\varepsilon 2} = 1.92, \quad C_{\varepsilon 3} = 0.8.$$

$R_f$ is the Richardson flux number used by Rodi [9]:

$$R_f = -\frac{G}{P+G}.$$

## 4. TURBULENCE MODEL FOR THE THERMAL FIELD

To obtain the turbulent heat flux, the hypothesis of a thermal eddy diffusivity is employed. This diffusivity is determined from a constant turbulent Prandtl number $Pr_t$:

$$\overline{u_i \theta} = -\alpha_t \frac{\partial \bar{T}}{\partial x_i} \tag{9}$$

where

$$\alpha_t = \frac{\nu_t}{Pr_t}.$$

The value 0.9 is frequently used for the turbulent Prandtl number. In this work we will show the results obtained with two other different turbulent Prandtl numbers, 0.35 (for the grid generated flow) and 0.4 (for the turbulent air jet).

4.1. *Equation for the variance of temperature fluctuations*

The equation for the variance of temperature fluctuations is obtained from the energy equation, with the Reynolds decomposition, taking the difference between the instantaneous and mean forms for the temperature:

$$\frac{D\overline{\theta^2}}{Dt} = \frac{\partial}{\partial x_j}\left(\alpha\frac{\partial \overline{\theta^2}}{\partial x_j} - \overline{u_j \theta^2}\right) - P_\theta - \varepsilon_\theta \tag{10}$$

where $P_\theta$ is the generation rate of $\overline{\theta^2}$ by mean temperature gradients:

$$P_\theta = -2\overline{u_j \theta}\frac{\partial \bar{T}}{\partial x_j}$$

and $\varepsilon_\theta$ is the dissipation rate of variance of temperature fluctuations:

$$\varepsilon_\theta = 2\alpha \overline{\frac{\partial \theta}{\partial x_j}\frac{\partial \theta}{\partial x_j}}.$$

As we are validating the model for turbulent flows, we are working with large Reynolds numbers ($\sim 10\,000$), thus the term due to molecular diffusion may be neglected [10]. The term of diffusion due to the turbulent convection is modeled with the first law gradient:

$$-\overline{u_j \theta^2} = C_\theta \frac{k^2}{\varepsilon}\frac{\partial \overline{\theta^2}}{\partial x_j}.$$

The value used for $C_\theta$ is 0.13 [11].

With the above hypothesis, the equation to be solved for the variance of temperature fluctuations is:

$$\frac{D\overline{\theta^2}}{Dt} = \frac{\partial}{\partial x_j}\left(C_\theta \frac{k^2}{\varepsilon}\frac{\partial \overline{\theta^2}}{\partial x_j}\right) - P_\theta - \varepsilon_\theta. \tag{11}$$

The term of dissipation rate of temperature fluctuations is modeled from the ratio of time scales of turbulent temperature and velocity field:

$$R = \frac{\overline{\theta^2}}{\varepsilon_\theta}\frac{\varepsilon}{k}. \tag{12}$$

Several studies have been realized in order to obtain the ratio $R$ from the grid generated flows. In ref. [5] a bibliographical review of the values found by several authors, in heated grid generated flows, is given. It shows that the values of the ratio $R$ can vary from 0.4 to 1.6 for the cases studied.

In this work we show a sensibility analysis of the value of the ratio $R$, within the usual values employed, over the level of the variance of temperature fluctuations for the turbulent air jet.

## 5. COMPUTATIONAL DETAILS

The finite volume method using the principle of a staggered mesh was applied to solve the set of equations presented above. In this method, the conservation equations are integrated in a control volume, and then the Gauss theorem is used to transform some integrals of volume into integrals of surface. All the scalar quantities are treated in the center of the control volumes and the velocities are localized in the center of the face of control volumes.

The equation of momentum conservation is discretized in time under semi-implicit form for the pressure gradient term. This method is derived from the SOLA method developed by Hirt *et al.* [4]. Below we show this discretization:

- conservation of mass:

$$\frac{\partial \overline{U}_i^{(n+1)}}{\partial x_i} = 0 \tag{13}$$

- conservation of momentum:

$$\frac{\overline{U}_i^{(n+1)} - \overline{U}_i^{(n)}}{\Delta t} + \left[\frac{\partial}{\partial x_j}(\overline{U}_i \overline{U}_j) - \frac{\partial}{\partial x_j}\left(v\frac{\partial \overline{U}_i}{\partial x_j} - \overline{u_i u_j}\right) - g_i(1-\beta(\bar{T}-\bar{T}^0))\right]^{(n)} + \frac{\partial \bar{P}^{(n+1)}}{\rho^0 \partial x_i} = 0$$

or in another form:

$$\overline{U}_i^{(n+1)} = \Delta t\left[S\overline{U}_i^{(n)} - \frac{\partial \bar{P}^{(n+1)}}{\rho^0 \partial x_i}\right]. \tag{14}$$

The method of solution consists in substituting the equation for the velocity at the time $n+1$ (equation (14)) in the equation of mass conservation at the time $n+1$ (equation (13)). With this method we can calculate the pressure field at the time $n+1$ and then the values of the velocities at the time $n+1$. The solution of the hydrodynamic problem is a field of pressure and velocity respecting the equations of mass and momentum conservation. To solve the linear system for the pressure the CHOLESKY method was used. It was possible to use this method because the matrix of this system is symmetrical, positive and entirely stocked in the computer memory.

For the equations of energy, $k$, $\varepsilon$ and the temperature fluctuations, we use the explicit scheme. The code used was TRIO/VF of the Centre d'Etudes Nucleaires de Grenoble, and the computer was a CRAY-1. The grid used had $(31 \times 32)$ points.

## 6. RESULTS AND DISCUSSION

The turbulent model shown in this paper has been applied to three kinds of configurations:

(a) isothermal grid-generated flow;
(b) grid-generated flow with cross-stream temperature gradient;
(c) fairly hot axisymmetrical turbulent air jet.

The comparison of the results, between the values obtained by the model and the measurements, is made for the stationary regime although the code can be used in a transitory regime. The first experiment (a) uses a grid with the mesh $B = 2.54$ cm, placed in a vertical wind tunnel. The test section has a length of 167 mesh and its cross-section is $16B \times 16B$. The mean speed of the air is 6.5 m s$^{-1}$. The Reynolds number based on the mesh is 10 000. The porosity of the grid is 0.66, made of square bars of $0.476 \times 0.476$ cm. The measured values for this experiment are given by Warhaft and Lumley [5]. Among the measures made by these authors we selected two cases: the first case with a mean temperature of 300 K and the second case with a mean temperature of 308 K.

We have used four types of boundary conditions to describe the experiment of grid-generated flows (experiments (a) and (b)). In the inlet of the computational domain ($Z/B = 80$), we have imposed the measured profiles of uniform velocity, temperature and turbulent quantities. For experiment (a), the values used for these boundary conditions were obtained from ref. [5]. For the hydrodynamic field, the values used are: vertical velocity $W = 6.5$ m s$^{-1}$, turbulent kinetic energy $k = 2.19 \times 10^{-2}$ m$^2$ s$^{-2}$ and the dissipation rate of kinetic energy of turbulence $\varepsilon = 9.51 \times 10^{-2}$ m$^2$ s$^{-3}$. For the thermal field the inlet boundary conditions are the following: In the first case, temperature $T = 300$ K and $\overline{\theta^2} = 4/72 \times 10^{-3}$ K$^2$ and in the second case, temperature $T = 308$ K and $\overline{\theta^2} = 1.22 \times 10^{-2}$ K$^2$.

In the center of the tunnel we have used a symmetrical condition, on the opposite side, an adiabatic wall. The logarithmic wall function was used [8]. In the outlet, we impose a nil pressure. Figure 1 shows these positions.

For the experiment (a), the production terms $P$ (due to the mean velocity gradient) and $G$ (due to the buoyancy) are nil. Thus, the terms due to convection and diffusion have an important role in the balance of $k$ and $\varepsilon$ equations. As there is no temperature gradient, it is possible to validate this model for the case when only the transport (convection, diffusion) and dissipation terms are taken into account in the temperature fluctuation equation (10). The values used for the ratio $R$ in the numerical model are the values found experimentally in ref. [5].

Figure 2 shows the results of the comparison

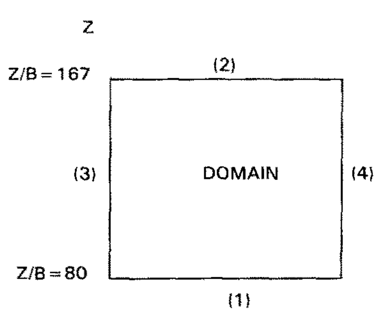


FIG. 1. Boundary conditions for the grid-generated flow. (1) Velocity and scalar quantities imposed. (2) Null pressure imposed. (3) Symmetry. (4) Adiabatic wall.

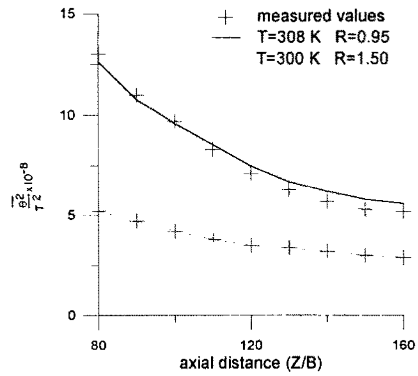


FIG. 2. Comparison between measured values presented in ref. [8] and calculation of the temperature fluctuations behind an isothermal grid.

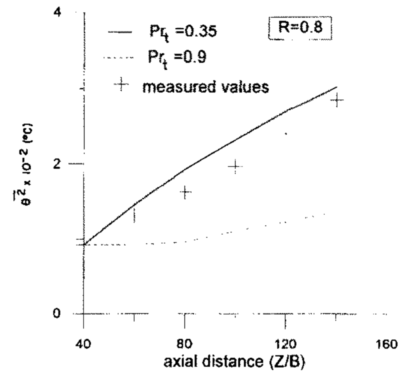


FIG. 3. Comparison between measured values [6] and calculations for a grid-generated flow with cross-stream temperature gradient.

between the calculations and measurements for the decay of temperature fluctuation, in the center of the wind tunnel for the first experiment (a). In this figure we notice the good agreement between calculations and measurements. We should remark that the only inconvenience of this model is the utilization of different values of $R$ (obtained experimentally) depending on the temperature, $R = 0.95$ for $T = 308$ K and $R = 1.5$ for $T = 300$ K. Although these temperatures are very similar, the values of the ratio ($R$) between the time scales of turbulent temperature and velocity field are very different. This occurs because of the large variation of the decay rate of temperature fluctuations. In grid turbulence, $R = n/m$, where $n$ and $m$ are the respective exponents of the power-law decays for velocity and temperature variance. In numerous experiments made by Comte-Bellot and Corrsin [12], in the grid-generated turbulence, it is shown that the decay exponent ($n$) in the decay law for the velocity fluctuations has a variation of about 12%. Nevertheless, measures made by Warhaft and Lumley [5] for the heated grid generated turbulence, show that the decay exponent ($m$) for the temperature fluctuations varies by a factor of more than 3. They [5] show that the decay rate of temperature fluctuations produced by heating the grid depends on the initial temperature fluctuations. Another phenomenon observed is that the wave number of the maximum temperature spectrum changes when varying the heat applied at the grid, indicating that the geometry of the thermal fluctuations was changed.

For the second experiment (b), we used the values obtained experimentally in ref. [6]. The only difference with the first experiment (a) was the imposition of a temperature gradient in the grid. This gradient was obtained by differently heating the bars of the grid. To make comparisons between the calculations and the measurements we chose a test with a mean speed of air of 3.4 m s$^{-1}$ (Reynolds number = 5200) and a temperature gradient of 8.1 K m$^{-1}$. For these experiments of grid-generated turbulence a order-of-magnitude analysis indicates that the buoyancy effects may be neglected. The values used for the inlet turbulent boundary conditions are: turbulent kinetic energy $k = 8.8 \times 10^{-3}$ m$^2$ s$^{-2}$, dissipation rate of kinetic energy $\varepsilon = 3.7 \times 10^{-2}$ m$^2$ s$^{-3}$ and temperature fluctuations $\overline{\theta^2} = 9.19 \times 10^{-3}$ K$^2$.

In Figs. 3 and 4 we show the results of the comparison between calculations and measurements, in the center of the wind tunnel, obtained for the second experiment (b). In this configuration all the terms of the temperature fluctuation equation (convection, diffusion, production due to the mean temperature gradient) play an important role. Figure 3 shows the results obtained using the ratio $R = 0.8$ and two values for the turbulent Prandtl number of 0.35 and 0.9. We verify that the value of 0.9 usually employed in several thermal turbulence models gives underestimated values of temperature fluctuations. The best agreement between calculations and measurements was obtained with $Pr_t = 0.35$. Using the value 0.9 for the turbulence Prandtl number we obtain smaller values of turbulent heat flux ($\overline{w\theta}$) than using 0.35 and consequently a smaller generation rate of temperature fluctuations. The velocity fluctuation $w$ is the component in the direction of the temperature gradient. The turbulent heat flux was correctly predicted when the value 0.35 was employed for the turbulent Prandtl number.

The values obtained for the dissipation rate of tem-

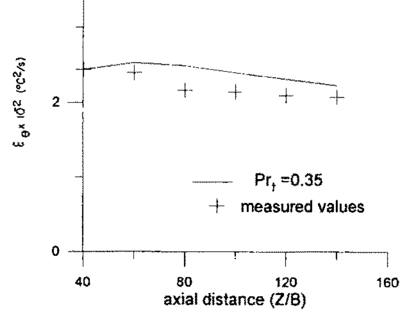


FIG. 4. Comparison between measured values [6] and calculations for the dissipation rate of temperature fluctuations.

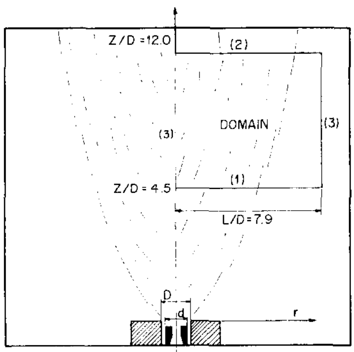


FIG. 5. Boundary conditions for the round jet. (1) Velocity and scalar quantities imposed. (2) Null pressure imposed. (3) Symmetry.

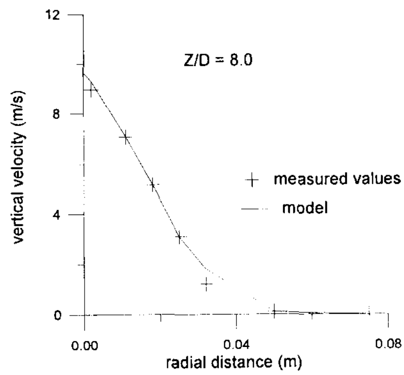


FIG. 6. Comparison between experimental data [7] and calculations for the vertical velocity ($Z/D$ = 8.0).

perature fluctuations are compared with the measured values and are presented in Fig. 4.

The turbulence model shown in this paper has also been applied to a fairly hot axisymmetrical turbulent air jet (Fig. 5). The experimental apparatus consists of an air jet that comes out of an annular tube with a mass rate of 15 $m^3 h^{-1}$. The inside diameter is $d$ = 18.2 mm and the outside diameter is $D$ = 25.3 mm. This flow is heated with electrical resistances placed downstream. The maximum difference of temperature, between the jet and the ambient temperature, is 22 K. For this experiment the role of buoyancy effects is small, but was considered in all calculations. The measured values are given in ref. [7]. In this experiment all the terms of the model play a part, because we have gradients of velocity, temperature and turbulent quantities. The computational domain and the types of boundary conditions are presented in Fig. 5. The values employed for the boundary conditions in the inlet of the domain are shown below in Table 1.

The values of mean velocity, $k$, $\varepsilon$, mean temperature and temperature fluctuations, given here for these boundary conditions, are measured values obtained from ref. [7].

The comparisons for the radial profiles of vertical velocities are presented in Figs. 6 and 7, respectively, for two sections $Z/D$ = 8.0 and $Z/D$ = 11.0. In these figures we note the good agreement obtained with the $k$–$\varepsilon$ model to predict the profile of mean vertical

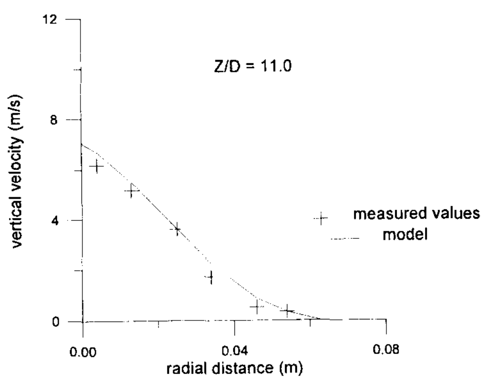


FIG. 7. Comparison between experimental data [7] and calculations for the vertical velocity ($Z/D$ = 11.0).

Table 1.

| $r$ (mm) | $W$ (m s$^{-1}$) | $T$ (K) | $k$ (m$^2$ s$^{-2}$) | $\varepsilon$ (m$^2$ s$^{-3}$) | $\overline{\theta^2}$ (K$^2$) |
|---|---|---|---|---|---|
| 1.1 | 14.3 | 307.2 | 8.6 | 2680.5 | 6.9 |
| 3.4 | 13.6 | 306.5 | 8.9 | 2090.0 | 7.1 |
| 5.6 | 12.5 | 305.5 | 9.7 | 2090.0 | 6.6 |
| 7.9 | 11.1 | 304.0 | 10.1 | 2101.0 | 5.6 |
| 10.2 | 9.5 | 302.5 | 10.3 | 2301.0 | 5.2 |
| 12.4 | 8.0 | 301.4 | 10.0 | 2270.0 | 5.0 |
| 14.7 | 6.2 | 300.0 | 9.1 | 2050.0 | 4.5 |
| 17.0 | 4.8 | 298.6 | 7.8 | 1670.0 | 4.2 |
| 19.2 | 3.5 | 297.3 | 6.7 | 1317.0 | 3.5 |
| 21.5 | 2.7 | 296.1 | 5.6 | 1037.0 | 2.7 |
| 23.7 | 2.2 | 295.0 | 4.6 | 762.0 | 2.0 |
| 26.0 | 1.7 | 294.8 | 3.6 | 563.0 | 1.8 |
| 28.3 | 1.4 | 293.7 | 2.7 | 368.0 | 1.7 |
| 30.5 | 0.9 | 293.3 | 2.2 | 270.0 | 1.5 |
| 33.2 | 0.4 | 293.0 | 1.0 | 140.0 | 1.3 |
| 36.4 | 0.2 | 293.0 | 0.5 | 50.0 | 0.8 |
| 41.1 | 0.2 | 293.0 | 0.3 | 26.0 | 0.5 |
| 47.38–185.0 | 0.2 | 293.0 | 0.1 | 3.0 | 0.2 |

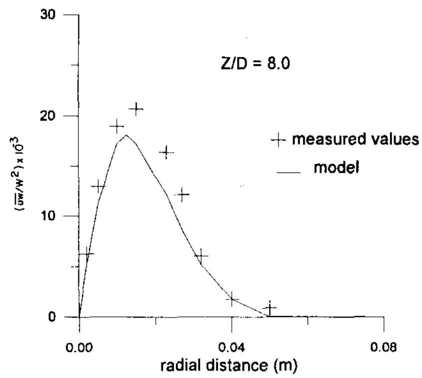


FIG. 8. Comparison between experimental data [7] and calculations for the Reynolds-shear stress ($Z/D = 8.0$).

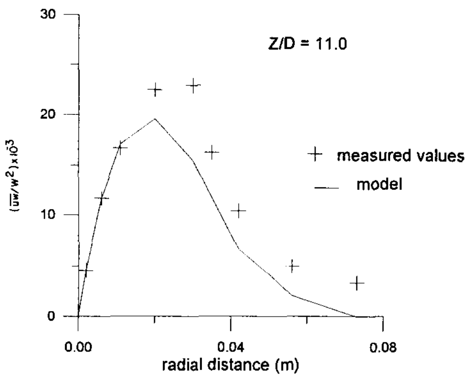


FIG. 9. Comparison between experimental data [7] and calculations for the Reynolds-shear stress ($Z/D = 11.0$).

velocity. The model predicts quite well the profile in the central region of the jet, but overpredicts it in the edge region (maximum deviation of about 25%).

Figures 8 and 9 show the comparison between the measured values and calculations for the component $\overline{uw}$ of the Reynolds stress. In these figures, we note that the model predicts the measured profiles, with a good agreement between the center of the jet and $r = 0.02$ mm and an underprediction beyond this distance. The maximum deviation is about 30%.

For the prediction of the mean temperature, we compare the use of two values for the turbulent Prandtl number, 0.9 and 0.4. In Figs. 10 and 11 we show the comparison between the model (with these two values of turbulent Prandtl number) and the measured values. The values of the mean temperature obtained with a turbulent Prandtl number of 0.9 (employed in several codes) are overestimated all over the region of the jet. When the value 0.4 is given to the turbulent Prandtl number, the level of temperature is correctly predicted between the central region of the jet and $r = 0.03$ mm, but is overpredicted in the edge of the jet.

Figures 12 and 13 show the results for the variance of temperature fluctuations in the two cross-sections,

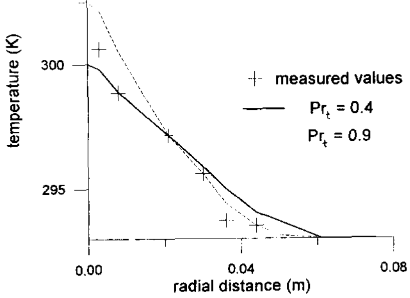


FIG. 10. Comparison between experimental data [7] and calculations for the mean temperature ($Z/D = 8.0$).

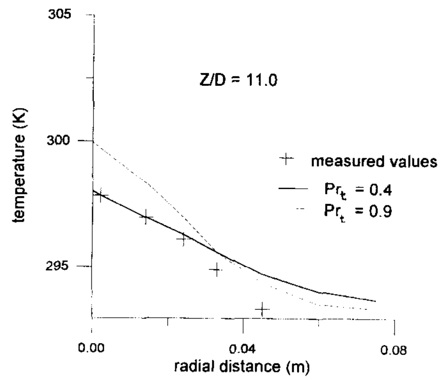


FIG. 11. Comparison between experimental data [7] and calculations for the mean temperature ($Z/D = 11.0$).

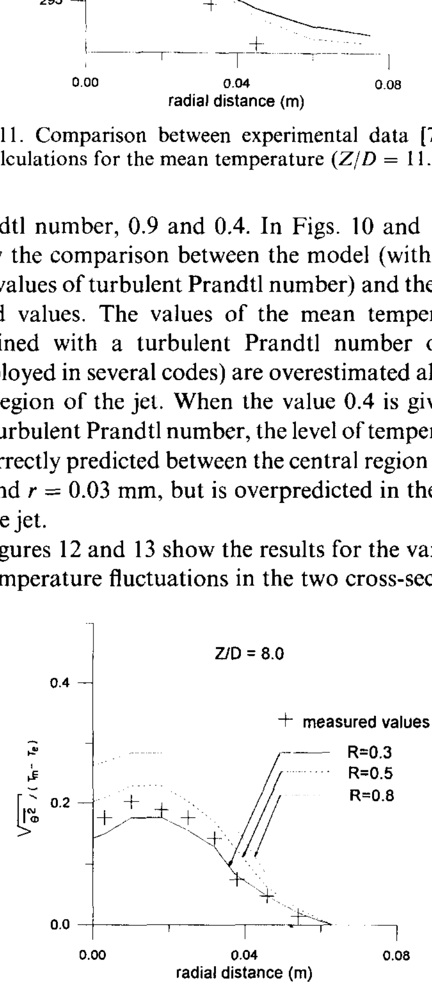


FIG. 12. Comparison between experimental data [7] and calculations for the temperature fluctuations ($Z/D = 8.0$).

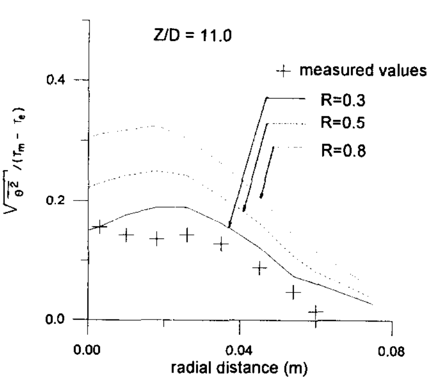


FIG. 13. Comparison between experimental data [7] and calculations for the temperature fluctuations ($Z/D = 8.0$).

$Z/D = 8.0$ and $Z/D = 11.0$, respectively. In these figures, we show the sensitivity of the ratio $R$, used to obtain the dissipation of the temperature fluctuations. We give three values for $R$: 0.3, 0.5 and 0.8. This range of values is found frequently in the literature. We note that the value 0.3 for $R$ gives the best agreement between calculations and measured values (for $Z/D = 8.0$ this value underpredicts the fluctuations and for $Z/D = 11.0$ this value overpredicts the temperature fluctuations). We observe that the more the values given to $R$ increase, the more the temperature fluctuations are overpredicted, because $R$ is inversely proportional to the dissipation rate of temperature fluctuations. The maximum deviation is about 20% when $R = 0.3$ is employed.

## 7. CONCLUSION

The three-equation model employed here has permitted us to calculate the turbulent thermal field for the grid-generated flows and turbulent round jets. We have shown the comparison between measurements and calculations for the variance of temperature fluctuations and its rate of dissipation, in flows behind a generated isothermal grid and with a cross-stream gradient temperature, in flows behind a generated isothermal grid and with a cross-stream gradient temperature. We have also shown the comparison between measured values and calculations for the mean velocity, mean temperature, Reynolds stress and variance of temperature fluctuations in a fairly hot axisymmetrical turbulent air jet. The results obtained with this model show a good agreement with the measured values. We notice that this agreement depends fundamentally on the values used for the constant models, ratio $R$ (for the temperature fluctuations) and the turbulent Prandtl number (for the mean temperature). In the case of grid generated flows that have been largely explored experimentally, measured values are available for these constants and there are good values to give to the necessary boundary conditions. This fact has enabled the validation of the model in the application of turbulence grid generated flows (isothermal and with a cross-stream gradient temperature).

The best agreement between calculation and measurements was obtained using the following values for $R$ and $Pr_t$ for the studied cases:

- isothermal grid-generated flow ($T = 300$ K)—$R = 1.5$,
- isothermal grid-generated flow ($T = 308$ K)—$R = 0.95$,
- grid-generated flow with cross-stream temperature—$R = 0.8$ and $Pr_t = 0.35$,
- weakly heated jet—$R = 0.3$ and $Pr_t = 0.4$.

The large variation of the ratio $R$ is related to the variation of the decay exponent for the temperature fluctuations. Warhalf and Lumley [5], in the grid generated turbulence, show that this variation occurs because this rate depends on the level of initial temperature fluctuations and the geometry of thermal fluctuations. Measurements show that the wave number of the maximum temperature spectrum changes with the heating applied to the grid.

We still have to work in the construction of refined turbulence models, mainly for the determination of the turbulent heat flux and for the dissipation rate of temperature fluctuations. The modelling of the equations for $(\overline{u_i\theta})$ and $(\varepsilon_\theta)$ and measurements of the different terms (diffusion, production and dissipation) of these equations have to be done for several flows. The knowledge of measured values for the boundary conditions and for the sections of the flows, will make it easier to determine the values employed for the constants of these models.

*Acknowledgements*—The author would like to thank Professor Denis Jeandeal, ECL, and Dr Dominique Grand, CENG, for many fruitful discussions. This work was financially supported by grants from CNPq (Brazil) and the computations by CEA (France).

## REFERENCES

1. B. E. Launder, *Heat and Mass Transport, Topics in Applied Physics, Turbulence* (2nd Edn) (Edited by P. Bradshaw), Chap. 6. Springer, Berlin (1978).
2. M. J. S. Lemos and A. Sesonske, Turbulence in combined convection in mercury pipe flow, *Int. J. Heat Mass Transfer* **28,** 1067–1088 (1985).
3. M. K. Chung and H. J. Sung, Four-equation turbulence model for prediction of the turbulent boundary layer affected by buoyancy force over a flat plate, *Int. J. Heat Mass Transfer* **27,** 2387–2395 (1984).
4. C. W. Hirt, B. D. Nichols and N. C. Romero, SOLA—numerical solution algorithm for transient fluid flow, Los Alamos Laboratory, Report LA-5852 (1975).
5. Z. Warhaft, and J. L. Lumley, An experimental study of decay of temperature fluctuation in grid-generated turbulence, *J. Fluid Mech.* **88,** 659–684 (1978).
6. A. Sirivat and Z. Warhaft, The effect of a passive cross-stream temperature gradient on the evolution of temperature variance and heat flux in grid turbulence, *J. Fluid Mech.* **128,** 323–346 (1982).
7. E. M. Bahraoui et L. Fulachier, Quelques résultats sur un jet turbulent axisymmétrique chauffé, *Journées d'Etude*, Institut de Mécanique Statistique de la Turbulence, Marseille, France (1985).
8. B. E. Launder and D. B. Spalding, The numerical computational of turbulent flow, *Comput. Meth. Appl. Mech. Engng* **3,** 269–289 (1974).
9. W. Rodi, Turbulence models and their application in hydraulics, *Int. Association for Hyd. Res.* Delft, The Netherlands (1978).
10. G. Mompean, Modélisation des écoulements turbulents avec transferts thermiques en convection mixte, Thèse de Doctorate, École Centrale de Lyon, France (1989).
11. D. B. Spalding, Concentration fluctuation in round turbulent free jet, *Chem. Engng Sci.* **26,** 95–107 (1971).
12. G. Comte-Bellot and S. Corrsin, The use of a contraction to improve the isotropy of grid-generated turbulence, *J. Fluid Mech.* **25,** 257–682 (1966).